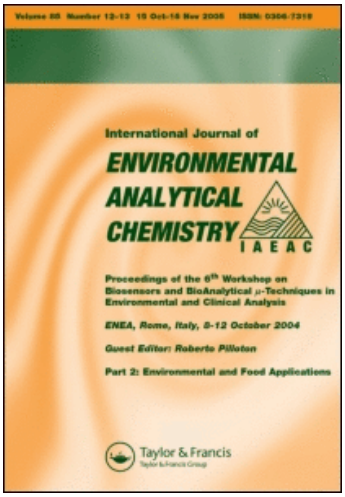

International Journal of Environmental Analytical Chemistry
Publication details, including instructions for authors and subscription information:
http://www.informaworld.com/smpp/title~content=t713640455

Profile of Aliphatic Hydrocarbons in a Recent Polynesian Microbial Mat

J. P. Boudou[a]; J. Trichet[a]; N. Robinson[b]; S. C. Brassell[b]
[a] Laboratoire de Géologie Appliquée, Université d'Orléans—C.N.R.S.—E.R.A., Orleans, France [b] University of Bristol—School of Chemistry, Organic Geochemistry Unit, Bristol, U.K

To cite this Article Boudou, J. P. , Trichet, J. , Robinson, N. and Brassell, S. C.(1986) 'Profile of Aliphatic Hydrocarbons in a Recent Polynesian Microbial Mat', International Journal of Environmental Analytical Chemistry, 26: 2, 137 — 155
To link to this Article: DOI: 10.1080/03067318608077110
URL: http://dx.doi.org/10.1080/03067318608077110

Intern. J. Environ. Anal. Chem., 1986, Vol. 26, pp. 137–155
0306-7319/86/2602-0137 $18.50/0

Printed in Great Britain

Profile of Aliphatic Hydrocarbons in a Recent Polynesian Microbial Mat

J. P. BOUDOU† and J. TRICHET

Université d'Orléans—C.N.R.S.—E.R.A. 601, Laboratoire de Géologie Appliquée, 45046 Orleans, France

and

N. ROBINSON and S. C. BRASSELL

University of Bristol—School of Chemistry, Organic Geochemistry Unit, Cantock's Close, Bristol BS8 1TS U.K.

(*Received February 20, 1985; in final form January 15, 1986*)

The extractable aliphatic hydrocarbon composition of four layers of a microbial mat from Hao atoll, French Polynesia, have been examined by GS-MS. These hydrocarbon distributions illustrate both the imprint of microbial populations on the lipid profiles and the selective diagenetic transformation of specific microbial lipids.

In the uppermost layer, principally composed of cyanobacteria, the *n*-alkane distribution is typical of such microbial origins, being dominated by C_{17}. With depth this *n*-alkane pattern is progressively changed by selective degradation of lower homologues. Thus, *n*-C_{31}, presumably derived from vegetation surrounding the pond, becomes the dominant component in the deeper layers. Also, C_{18} and C_{19} methyl mid-chain branched alkanes appear to persist with depth relative to their linear analogues, indicating their preferential survival, or liberation from bound lipids.

A number of alkenes (e.g. C_{17}, C_{29}, C_{31}) appear to be associated with either the upper cyanobacterial, or underlying photosynthetic bacterial, horizons. They decrease markedly in concentration in the deeper layers, showing an enhanced degradation relative to *n*-alkanes of the same carbon number.

---

†Present address: Université Pierre et Marie Curie—C.N.R.S. L.A. 191, Laboratoire de Géochimie et Métallogénie, 4 Place Jussieu, 75252 Paris, Cedex 05, France.

Δ^2-Sterenes occur in the layers and presumably arise from dehydration of steroidal alcohols. The distribution of these sterenes appears to indicate a selective dehydration of C_{27} components.

In addition, a "hump" corresponding to unresolved components of alkenyl character is observed in the subsurface photosynthetic bacterial layer, indicating that such phenomena can be of natural, as well as pollutant anthropogenic, origin.

KEY WORDS: Aliphatic hydrocarbons, microbial mat, GC-MS, hydrocarbon profile.

INTRODUCTION

Microbial mats are of considerable geological significance as they represent the closest modern counterparts of the precambrian stromatolites. Thus, the study of living microbial mats can give valuable insight into environmental conditions which prevailed in Precambrian times. Also, the individual microbial layers of such mats tend to be populated by specific organisms (e.g. cyanobacteria, purple photosynthetic bacteria) so that differences in the organic matter of the various horizons of the mat can be assessed in terms of the influence of these different microorganisms. In addition, microbial mats represent an example of the role that microorganisms can play in mineral accumulation.

In order to determine the significance of chemical fossils found in precambrian stromatolites, extensive gas chromatography-mass spectrometry (C-GC-MS) analyses have been performed on the lipids of distinct strata of various contemporary microbial mat systems. These analyses of lipids have represented a new approach in the investigation of the environmental biogeochemistry of modern stromatolites. They have shown that the organic components of microbial mats can be correlated to a certain extent with those observed in isolated and cultured living algae and bacteria from marine and freshwater environments, and to a more limited extent, with those from Precambrian stromatolites.[1]

In this paper we report the C-GC-MS analyses of extractable (non-volatile) hydrocarbon composition of sediment in four layers of a microbial mat from Hao, French Polynesia.[2] The imprint of microbial populations on the lipid profiles and the microbial transformations of these lipids are discussed.

ENVIRONMENTAL DESCRIPTION OF THE H12 MICROBIAL MAT OF HAO

In Polynesia, microbial mats are found in ponds of several hundred square meters in size on the emerged parts of atolls, "motus" in Polynesian. These ponds originate from either the closing of depressions (ancient passages between the open sea and the lagoon of interdune zones) by sand deposits of the uplift of the atoll relative to the sea level. The average depth of the ponds is 1 meter. Their waters are connected to the non-marine water table (Ghyben–Herzberg lens[2]) and also receive rain water and some sea-water entering the pond essentially from sea spray.

Variations in the relative amounts of the waters supplied from these sources and to the biogeochemical processes in action inside sediments,[3,4] lead to fluctuations in the salinity of the interstitial solutions. In this respect, these Polynesian cyanobacterial mats differ from the saline or hypersaline cyanobacterial deposits described elsewhere.

General features of the sedimentation and the organic geochemistry of such mats have been firstly studied in Mururoa in Tuamoto archipelago (Figure 1),[2,5,6] Trichet *et al.* (unpublished), and more recently, in the H12 pond of Hao.[3,4]

The sedimentary and biogeochemical patterns encountered in H12 pond of Hao, like the other Polynesian small basins where microbial mats are characterized by organic matter essentially produced by cyanobacteria and other bacteria. The living cyanobacteria (mainly *Phormidium fragile, Lyngbia confervoides, Lyngbya aestuarii, Aphanocapsa*) are located in the uppermost centimeter of the sedimentary profile (Figure 2).[3] Between this green cyanobacterial layer and the top of the red coloured sediment layer where decomposition and diagenesis of organic matter occur, a 1–3 cm thick pink to purple layer is often observed. Its colour arises from pigmented photosynthetic purple bacteria. The lower sediments display a red colour due to abundant carotenoid pigments, which might come from the degradation of photosynthetic bacterial cells (Trichet, unpublished data). The upper photosynthetic layers contain 6.10^5 bacteria per ml of sediment (95% are aerobic), whereas the red layers contain 2.10^5 bacteria per ml of sediment of which 60% are aerobic.[3] Thus, there is

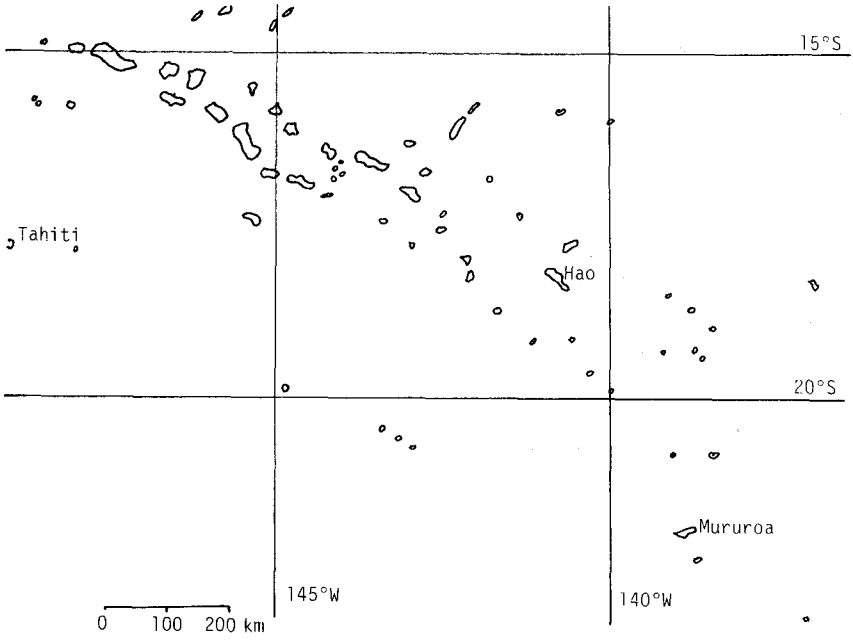

FIGURE 1 Location of Hao atoll in the Tuamotu archipelago (French Polynesia).

a clear difference in the aerobic character of the sedimentary bacteria with depth.

The variations with depth in the salinity, pH, Eh, dissolved oxygen of interstitial water and organic carbon content of sediment with depth are shown in Figure 2. In the upper living photosynthetic layer, pH is high, up to 9.1, and the Eh variation curve also shows a peak at this level due to O_2 production. The reducing layers are marked by a sharp decrease in pH of interstitial water, being due to the bacterial production of H_2S and CO_2 by sulfate-reduction.[3]

Biogeochemical reactions cause the precipitation of high Mg-calcite (12 to 19% moles $MgCO_3$) in the sediments, where association of *Lyngbia* with calcite rich layers is particularly noticeable. The location of the calcite crystal is controlled by the fine structure of the sediments, which in bulk terms can be regarded as protostromatolitic.[3,4]

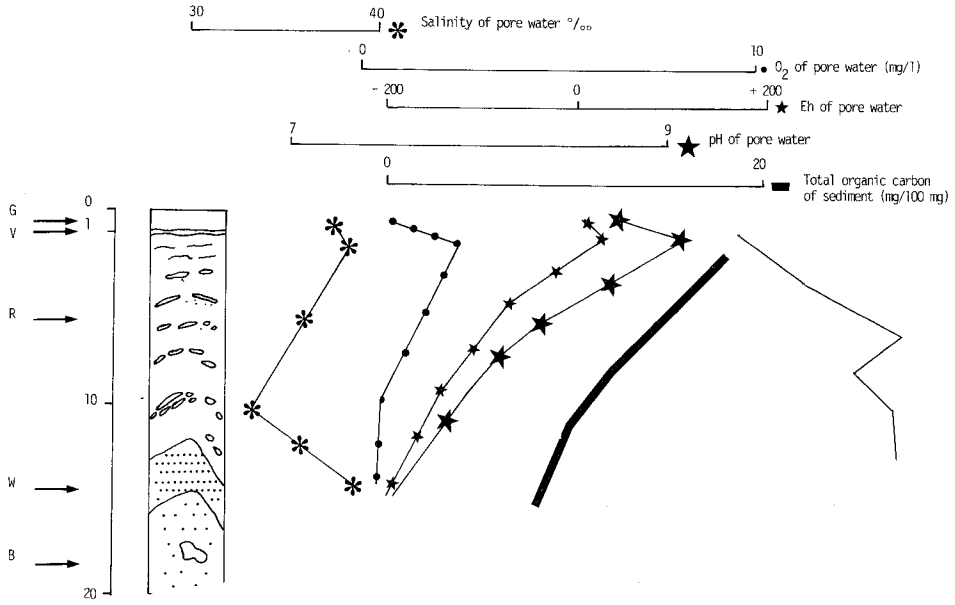

FIGURE 2 Depth profile of lithology, pore water chemistry and organic carbon content of sediment in the microbial mat of the H12 pond of Hao atoll. (G = Living green cyanobacteria, V = pigmented photosynthetic purple layer, R = Red organic layer including laminar and granular calcite deposits, W = White detritic sand, B = This layer, above the coral rock, is around 10 cm thick. It is a mixture of grey detritic sand and organic matter. Redrawn from Trichet, Boudou, Chichereau, Kergonou (unpublished) and from Defarges.[16]

EXPERIMENTAL PROCEDURES

The sediment samples studied here were collected from pond H12 of Hao.[3] A tube was used to take a 15 cm core which was kept in a nalgene container with a screw cap, refrigerated at +4°C. No visible micromorphological alterations were observed during storage.[3]

The core sample was divided into four sections which were freeze dried:

1. Section G: a green layer containing cyanobacteria (1.0–1.2 cm, organic carbon content: 14.5%).

2. Section V: a pink-violet layer containing pigmented bacteria (1.0–1.2 cm, organic carbon content: 21.7%).

3. Section R1: upper part of the red sediments (1.2–4.5 cm, organic carbon content: 15.1%).

4. Section R2: lower part of the red sediments (4.5–12 cm, organic carbon content: 12.7%).

All solvents used for extraction, fractionation and dilution were checked for contaminants and showed no significant peaks in blank analysis. The freeze dried samples were extracted ($CHCl_3$/MeOH, 1:5.5) by ultrasonication and hydrocarbon fractions were separated from these total lipid extracts using an alumina column with hexane as eluant.

Hydrocarbons were analysed by gas chromatography (GC) and computerised GC-mass spectrometry (C-GC-MS). GC analysis, using on column injection, was carried out on an Erba Science 4160 instrument fitted with an open tubular flexsil (25 cm × 0.3 mm i.d.) column, wall coated with OV-1.

A typical run was programmed from 60°C to 280°C at 4°C mm^{-1} and held isothermally at 280°C. H_2 was used as carrier gas. C-GC-MS analyses were performed on a Finnigan 4000 mass spectrometer coupled to a Finnigan 9610 gas chromatograph with on-line INCOS 2300 data system.[7] GC conditions were similar to those described above, with the column leading through a heated interface box into the ion source of the mass spectrometer. Typical MS operating conditions were: mass spectra were collected every second from 50 to 550 mass units, with an emission current of 350 μA, a 35–40 eV electron energy, an accelerating voltage of 1700–1750 V, and an ion source temperature of 250°C.

Hydrocarbon identifications were based on a combination of mass spectral interpretation, comparison with standard and relative retention times, or with mass spectra of standard compounds and by coinjection with reference compounds. Where M^+ ions were of low abundance, mass chromatography was used to aid compound identifications.

Hydrocarbons were quantified from their GC responses by comparison of their peak areas with that of a known quantity of an external standard. The FID did not show significant variation in sensitivity towards the different hydrocarbon standards used, and equal response factors were assumed for standard and sample quantification. Where peaks were insufficiently resolved to permit

accurate quantification from GC, approximate quantification was made from mass chromatograms of characteristic ions in the mass spectra of the components. The inherent difficulties in accurately measuring small amounts of compounds in complex mixtures limit the usefulness of absolute quantification; hence, such quantitative data are best employed for comparative purposes.

Quantification of the "humps" observed in the hydrocarbon chromatograms is difficult because of their unresolved character; their areas were therefore measured to provide a basis for intersection comparisons.

RESULTS

In the analysis of the hydrocarbon composition of the sections of H12 microbial mat, 23 alkanes and 43 alkenes were identified (Table 1 and 2), namely:

—*n*-alkanes ranging from *n*-C_{16} to *n*-C_{33}, various branched alkanes (7-methylheptadecane), 3-methylheptadecane, 7-methyldecane, 6-methyloctadecane, and 4-methyloctadecane).

—Some different 28 *n*- and branched alkenes (ranging from C_{17} to C_{31} with 1 to 5 unsaturations), 6 acyclic isoprenoid alkenes (3 phytenes, a phytadiene and two isomeric forms of squalene), 4 unsaturated steroids (C_{27}–C_{29}) and 5 hopenes (C_{29}, C_{30}).

The total reconstituted ion current traces from capillary GC-MS of the total hydrocarbon fractions from the four sections of the microbial mat are shown in Figure 3. Each shows a pattern with a bimodal distribution. Despite the use of high resolution GC, the chromatograms show "humps" of variable intensity in the range *n*-C_{15}–*n*-C_{25}. In V the "hump" is composed of an unresolved complex mixture of alkenyl compounds and polymeric sulphur, as seen as by comparison of the RIC and the mass chromatograms (Figure 4) for m/z 85 (alkanes), 83 (alkenes), 81 (alkadienes) and 64 (S_6, S_7, S_8). In Figure 3 the area of this "hump" appears to increase sharply from the G layer to the V layer and the decrease in the lower R1 and R2 core sections.

n-Alkanes and branched alkanes (Table I) were detected in the mass fragmentogram m/z 85. Branched alkanes are tentatively

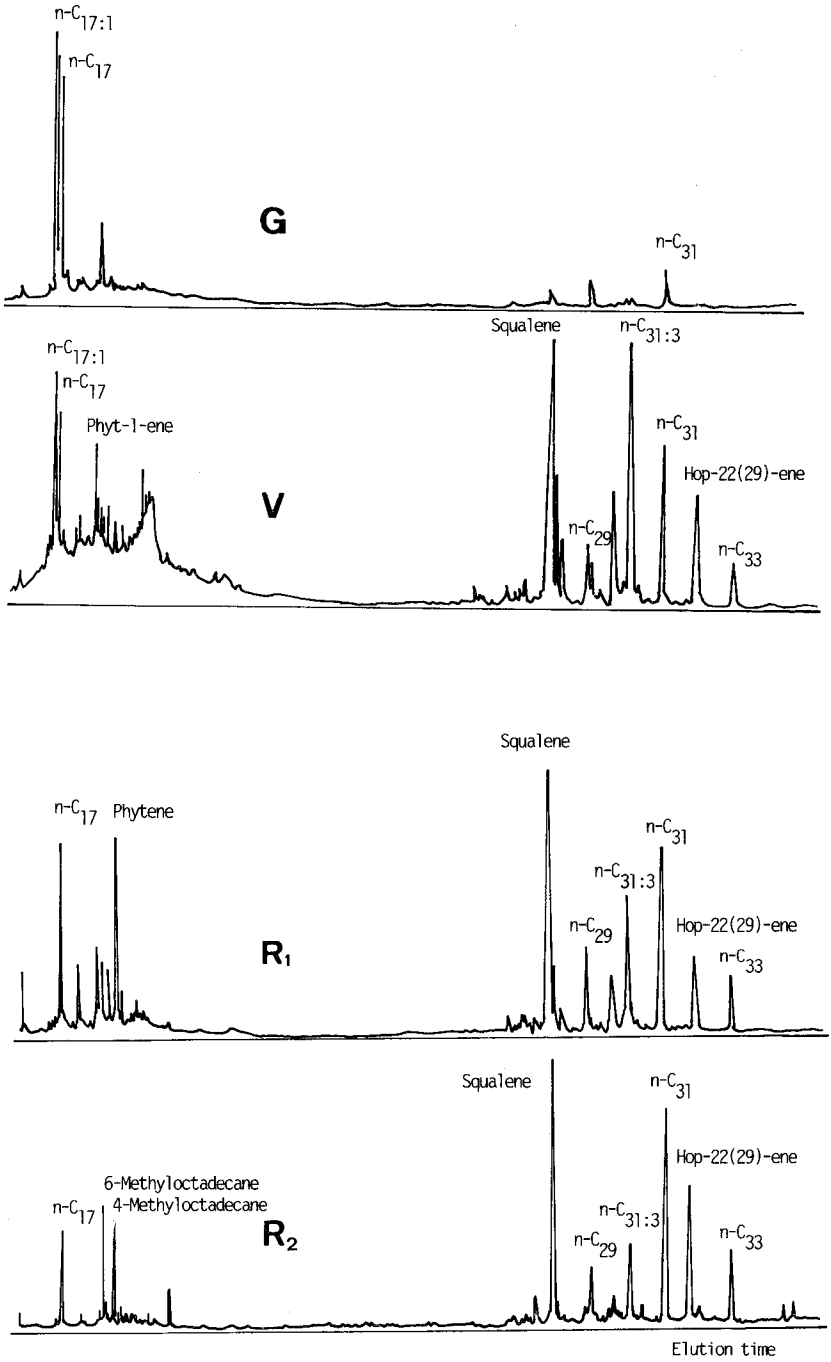

FIGURE 3 Total reconstituted ion chromatograms (RIC) from C-GC-MS of the extractable hydrocarbons of core sections: G, V, R1, R2, from the microbial mat of Hao atoll.

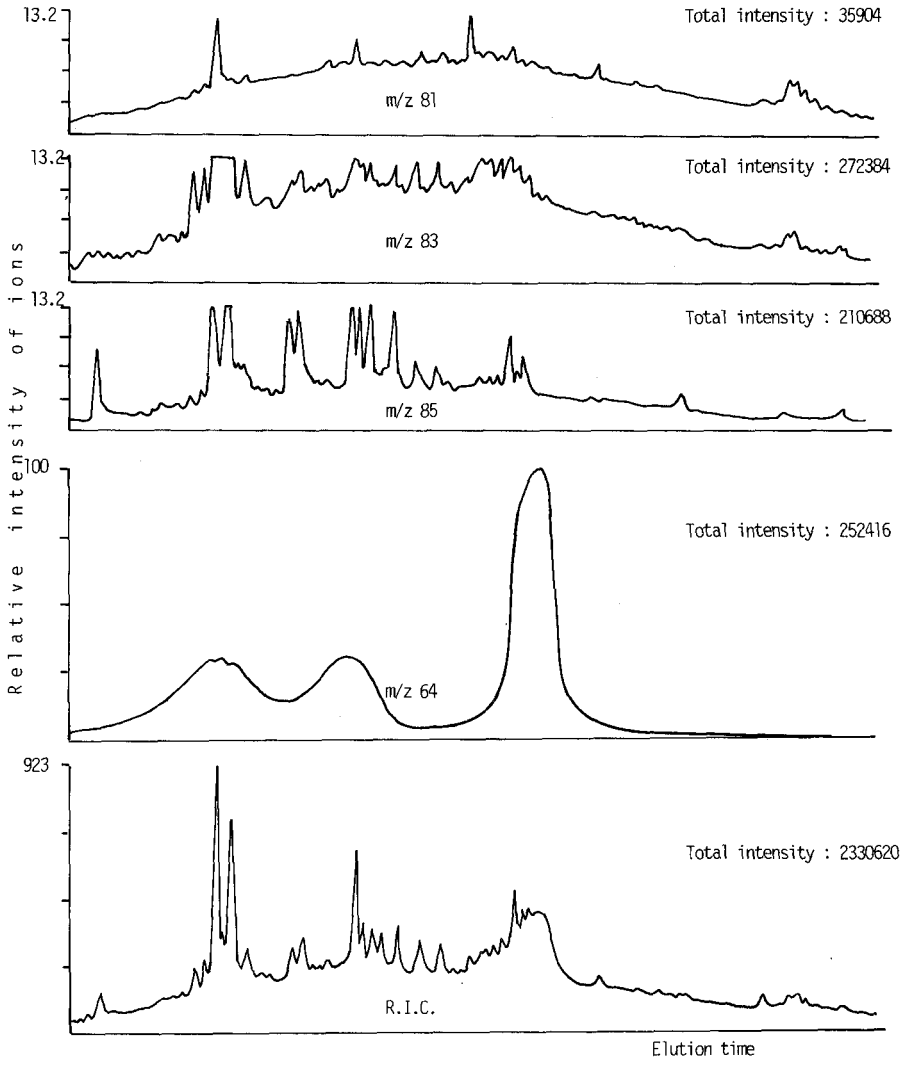

FIGURE 4 Partial RIC and partial mass fragmentograms for the hydrocarbon "hump" from section V. (a) m/z 81, 83, 85 (direct response: relative intensity of ions normalized to the total intensity) (b) m/z 64 and R.I.C. (relative intensity of ions normalized to the highest peak).

TABLE I

Straight and monomethyl branched chain hydrocarbons in the H12 microbial mat of Hao atoll (hydrocarbons are presented by elution order and the concentrations are expressed in μg/g dry wt.)

Component	Structure (Figure 6)	Method of identification	G	V	R1	R2
			μg/g dry wt. sediment			
Hexadecane		GC+MS	10	10	12	8
Hexadecene	(16:1)	MS	1	nd	nd	nd
Heptadecene′	(17:1)	MS	1	8	1	nd
Heptadecene″	(17:1)	MS	176	9	4	nd
Heptadec-1-ene	(A)	MS	168	97	2	0.5
Heptadecene	(17:1)	MS	8	9	4	tr
Heptadecane		GC+MS	156	90	76	40
Heptadecene	(17:1)	MS	11	8	4	tr
7-Methylheptadecane	(B)	MS	3	9	18	8
3-Methylheptadecane	(C)	MS	3	8	7	1
7-Methyloctadecane	(D)	MS	nd	nd	nd	8
Octadecene	(18:1)	MS	nd	5	3	nd
6-Methyloctadecane	(E)	MS	nd	18	10	51
Octadecadiene	(19:2)	MS	2	nd	nd	nd
Octadecane		GC+MS	39	18	21	12
4-Methyloctadecane	(F)	MS	nd	22	18	41
Eicosapentaene	(20:5)	MS	nd	7	nd	nd
Nonadecene	(19:1)	MS	nd	5	tr	nd
Nonadec-1-ene	(19:1)	MS	nd	22	tr	nd
Eicosadiene	(20:2)	MS	tr	nd	nd	nd
Nonadecane		GC+MS	tr	4	2	3
Eicosane		GC+MS	tr	3	1	2
Heneicosadiene	(21:2)	MS	nd	3	nd	nd

Heneicosane		GC+MS	tr	2	0.5	0.5
Docosane		GC+MS	tr	0.5	0.3	0.5
Tricosane		GC+MS	tr	0.5	0.3	1
Tetracosane		GC+MS	tr	1	0.3	1
Pentacosane		GC+MS	tr	2	1	3
Hexacosene	(26:1)	MS	nd	2	0.2	0.4
Hexacosadiene	(26:2)	MS	nd	2	0.2	0.4
Hexacosane		GC+MS	tr	9	1	3
Heptacosadiene	(27:2)	MS	nd	4	1	1
Heptacosene	(27:1)	MS	nd	8	2	1
Heptacosane		GC+MS	0.5	11	8	7
Octacosene	(28:1)	MS	nd	12	8	6
Octacosadiene	(28:2)	MS	nd	10	8	3
Octacosane		GC+MS	1	13	9	9
Nonacosatriene	(29:3)	MS	nd	106	34	6
Nonacosene	(29:1)	MS	nd	15	6	3
Nonacosadiene	(29:2)	MS	nd	37	11	4
Triacontadiene	(30:2)	MS	nd	3	nd	nd
Nonacosane		GC+MS	28	48	45	40
Triacontatriene	(30:3)	MS	nd	32	5	3
Triacontene	(30:1)	MS	nd	2	1	nd
Triacontadiene	(30:2)	MS	nd	9	2	0.5
Triacontane		GC+MS	2	12	10	9
Hentriacontatriene	(31:3)	MS	3	200	92	45
Hentriacontadiene	(31:2)	MS	nd	7	1	tr
Hentriacontane		GC+MS	35	169	127	136
Dotriacontane		GC+MS	1	13	10	9
Tritriacontane		GC+MS	2	40	38	42
TOTAL			650	1121	597	500

nd = not detected, tr = present in trace amounts ($\ll 1\ \mu g/g$).

assigned from the fragment ions, indicating methyl substitution (cf. no pristane of phytane was identified in any of the samples, neither were any polycyclic alkanes, e.g. steranes, hopanes).

Alkanes were not isolated (e.g. by Ag^+ TLC) from total extractable hydrocarbons prior to high resolution capillary GC-MS to avoid possible discrimination during fractionation. *n*-Alkenes were tentatively identified from their mass spectra, principally from their molecular ions and the abundance in the mass spectrum of the $C_nH^+_{2n-1}$ ion series. The double bond position of such compounds, except for 1-alkenes, cannot be determined from their spectra.

The only branched chain unsaturated hydrocarbons recognised were isoprenoids. Phytenes and phytadienes were identified by comparison of their mass spectra with reference compounds (e.g. for phyt-1-ene and phyt-2-ene). Squalene was discriminated from its isomer on GC retention time data.

The polycyclic hydrocarbons recognised were sterenes and hopenes, Δ^2-sterenes were recognised by mass chromatography of m/z 215 and $[M-54]^+$.

Hopenes were observed in mass chromatograms of m/z 191 and their assignments are based on comparison of their mass spectra and retention times with those of authentic standards.

The depth profile of the concentrations of all the hydrocarbon is presented in Tables I and II. The changes with depth in the concentrations of hydrocarbons and in selected hydrocarbon ratios are shown in Figure 5. The hydrocarbon concentrations (expressed as per thousand of the total organic carbon) increase from 4.7, in the freshly deposited cyanobacteria layer, to 7.5 in the underlying photosynthetic bacterial layer, then decrease to 6.3 in the lower anaerobic layers. In contrast, concentrations expressed as a percentage of the total extractable lipids identified (hydrocarbons + esters + acids + alcohols + ketones) increase appreciably from 16 in the upper two layers to 27 in the bottom section.

In the cyanobacterial layer (G) the hydrocarbon distribution is simple, almost unimodal and maximises at n-C_{17} for alkanes and alkenes. In this sample the odd/even predominance of the higher *n*-alkenes (n-C_{26} to n-C_{33}) is greater than 8. This pattern changes in lower sections as the ratio between the second mode (n-C_{26} to n-C_{33}) and the first mode (C_{16} to C_{25}) increases, as exemplified by the n-C_{31}/n-C_{17} ratio (Figure 5), with the *n*-alkanes and *n*-alkenes

TABLE II

Isoprenoid hydrocarbons in the H12 microbial mat of Hao atoll (acyclic isoprenoids, steroids and hopanoids are presented by elution order and the concentrations are expressed in μg/g dry wt.)

Component	Structure (Figure 6)	Method of identification	G	V	R1	R2
			μg/g dry wt. sediment			
Phyt-1-ene	(G)	MS	nd	59	21	tr
Phytene	(20:1)	MS	nd	16	118	6
Phyt-2-ene	(H)	MS	nd	15	15	3
Phytadiene	(20:2)	MS	*tr*	3	9	*nd*
Squalene isomer		GC+MS	nd	10	nd	nd
Squalene	(I)	GC+MS	16	281	172	170
Cholest-2-ene+	(J)	GC+MS	nd	nd	3	11
Cholesta-3,5-diene	(K)	GC+MS				
24-Methylcholest-2-ene	(L)	GC+MS	nd	nd	nd	tr
24-Ethylcholest-2-ene	(M)	GC+MS	nd	nd	tr	2
30-Norhop-17(21)-ene	(N)	GC+MS	nd	nd	nd	9
Hop-17(21)-ene	(O)	GC+MS	10	nd	nd	5
Neohop-13(18)-ene	(P)	GC+MS	0.5	4	3	3
Hop-22(29)-ene	(Q)	GC+MS	7	110	61	104
Hop-21-ene	(R)	GC+MS	4	nd	nd	tr
TOTAL			37	498	412	304

nd = not detected, tr = present in trace amounts ($\ll 1$ μg/g).

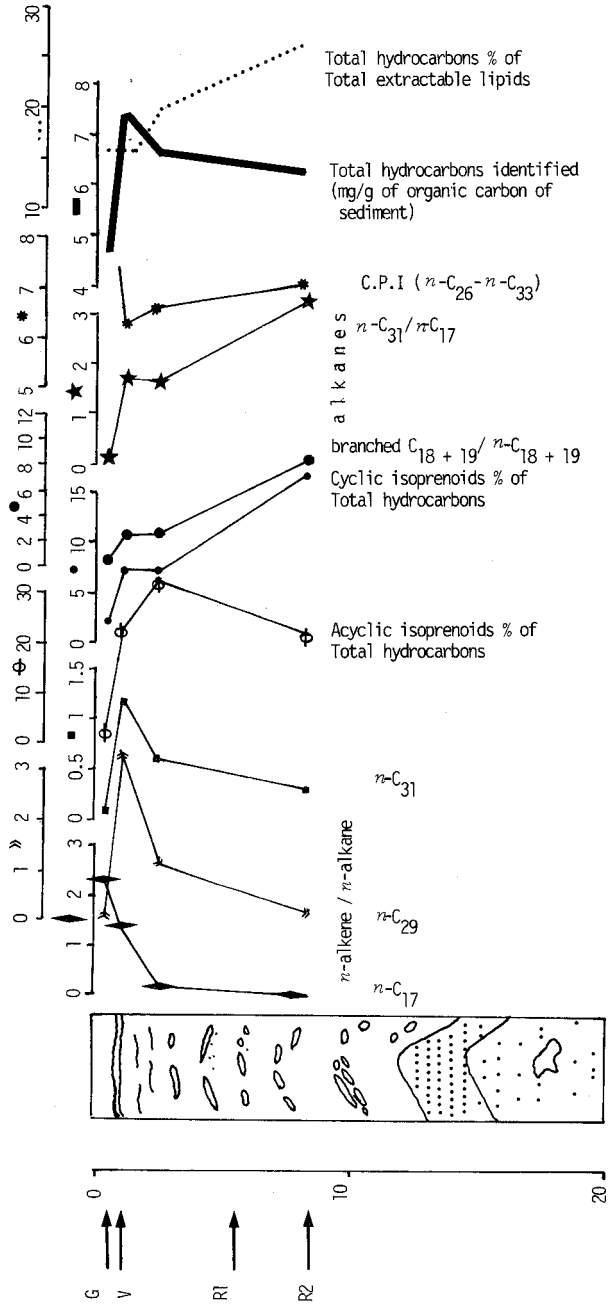

FIGURE 5 Depth profile of extractable hydrocarbon concentrations and selected ratios in the microbial mat of Hao atoll. Plots are drawn from the mid-depths of each core section.

increasingly maximising at n-C_{31}. The CPI of n-alkanes identified are C_{18} and C_{19} components. Progressively they become the major hydrocarbons in the first mode as illustrated by changes in the ratio of branched C_{18+19}/n-C_{18+19} with depth (Figure 5). Unsaturated hydrocarbons (C_{29}, C_{31}, phytenes) concentrations increase from the G layer to the V layer then decrease markedly like n-$C_{17:1}$ below this layer.

A further feature of the mat sequence is the clear increase of polycyclic structures with depth.

DISCUSSION

As expected, the upper green layer shows a high algal contribution typical of cyanobacteria with n-C_{17} as the predominant alkane. Lower concentrations of higher homologues, maximising at n-C_{31}, are present with a high odd/even predominance. There is strong odd/even dominance (CPI) throughout the mat sequence, which is typical of the n-alkane distributions of higher plants. The presence of such plants close to those Polynesian microbial mats tends to support this hypothesis.

In the lower levels of the microbial mat profile of Hao, the n-C_{31} alkane becomes dominant, presumably due to an increased higher plant contribution in the past or the preferential microbial degradation of lower homologues, notably n-C_{17} in the aerobic G and V layers. A similar feature was observed in Laguna Guerrero Negro.[8]

In the Hao microbial mat, like many other recent sediments, a similar distribution for n-alkenes and n-alkanes is observed. It is probable therefore that they originate from the same sources, although other origins for n-alkenes are possible: the abundance of the n-alkenes in the V layer and their decrease in the R1 and R2 layers, suggest that they either originate from bacteria or are rapidly degraded by bacteria.

The presence of mid-chain methyl branched alkanes found in the upper G layer (Table I) is consistent with their biological occurrence in cyanobacteria. The increase in these branched components with depth (Figure 5) may be due to their resistance to degradation relative to n-alkanes and n-alkenes.

The microbial mat from Hao differs from other microbial mats in

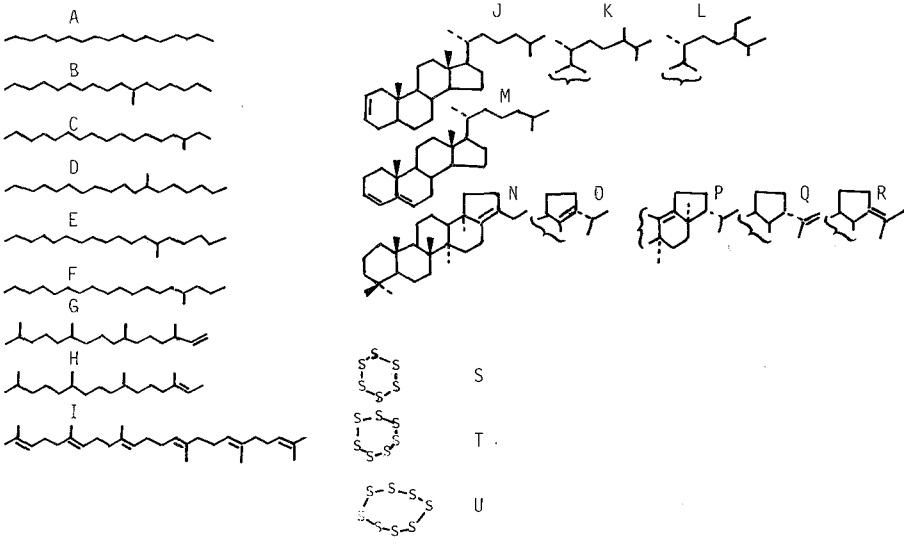

FIGURE 6 Structures of hydrocarbons listed in Tables I and II, and structures of some sulphur compounds associated with extractable hydrocarbons.

(A = Heptadecene, B = 7-Methylheptadecane, C = 3-Methylehaptadecane, D = 7-Methyloctadecane, E = 6-Methyloctadecane, F = 4-Methyloctadecane, G = Phyt-1-ene, H = Phyt-2-ene, I = Squalene, J = Cholest-2-ene, K = Cholesta-3,5-diene, L = 24-Methylcholest-2-ene, M = 24-Ethylcholest-2-ene, N = 30-Norhop-17(21)-ene, O = Hop-17(21)-ene, P = Neohop-13(18)-ene, Q = Hop-22(29)-ene, R = Hop-21-ene, S, T and U = Polymeric sulfur).

that pristane and phytane are absent in all the sections. For the G layer this observation is consistent with the reports of their non-occurrence in cyanobacteria.[9,10] In the V and R1 layers of the microbial mat (Table II) phytenes appear as major components and small amounts of a phytadiene are observed. These data suggest that these components are associated with bacteria, either as their biosynthetic or degradative products.

Squalene is present in all the mat layers. This occurrence suggests that squalene may originate from both cyano- and other bacterial sources, with the latter markedly more important. An isomeric squalene (Table II) was also recognised in V. This component probably arises from bacteria, perhaps archaebacteria.

Sterenes are widely distributed in the lower levels of microbial mats from many locations. They are diagenetic products, possibly generated by microbial action, hence their absence in the living mat layer. The microbial mat from Hao contains, in the R horizon C_{27}, C_{28} and C_{29} Δ^2-sterenes, with the first markedly more abundant (Table II). These components are presumably formed as dehydration products of 5α (H)-stanols, a suggestion by the observed similarity in the sedimentary 5α (H)-stanols and Δ^2-sterenes distributions.[11] As in Solar Lake,[12,13] cholestene is the dominant skeleton, supporting the possibility of preferential degradation of C_{27} sterols in microbial mat systems.

Hop-22(29)-ene is an abundant alkene constituent of *Lyngbia aestuarii*[14] and occurs in mats populated by this cyanobacterium, e.g.[8] It is a dominant triterpene in the microbial mat from Hao, where *Lyngbia aestuarii* and *L. confervoides* are abundant throughout the profile in association with calcite rich layers.[3] Hop-22(29)-ene is, however, markedly higher in concentration in the V layer than in the G layer, suggesting that non-cyanobacterial bacteria are the source of this compound in the mat sequence. Hop-21-ene is a minor component of the mat (Table II). Hop-17(21)-ene is present in the G layer. Presumably it originates from cyanobacteria, although it has yet to be identified in these organisms. In contrast to Laguna Guerrero microbial mat,[8] there is no clear diagenetic trend in the triterpenoid distributions.

UCMs are commonly composed of unresolved branched and cyclic hydrocarbons, as seen from the mass fragmentograms for alkenyl and alkanyl ions (Figure 4).

Sediments remote from anthropogenic sources of hydrocarbons do not generally contain a UCM. Non-anthropogenic origins for a UCM are, however, possible. For example, a natural input of hydrocarbons from the weathering of sedimentary rocks has been suggested to explain UCMs in the range C_{15}–C_{25}, as well as pristane and phytane, in early post-glacial sediments of Greifensee.[15] A UCM is observed in the hydrocarbon distributions of some anaerobic non-photosynthetic bacteria and green algae,[9,16] although laboratory contamination cannot be excluded in these instances. A "hump" in the C_{17}–C_{26} region has also been found for the decomposition products of soil micro-organisms in culture.[17] Perhaps such a feature may therefore represent the anaerobic decomposition products of

algae and bacteria. The "hump" observed in the GC of the total hydrocarbons of the V layer from the Hao microbial mat (Figures 3, 4) is associated with an abundance of higher *n*-alkanes with a high CPI and does not co-occur with any traces of pristane or phytane. It therefore appears that this "hump" is natural and comes from the intense bacterial activity which occurs at this level. A similar feature has been observed in Chilean paraffin dirt.[18]

CONCLUSIONS

Examination of the extractable aliphatic hydrocarbon composition of four layers of the microbial mat from Hao has revealed:

1. Many similarities to the characteristic features of other microbial mat systems.

2. A direct relationship between many of the compounds identified and their biological sources, notably cyanobacteria, photosynthetic bacteria and higher plants.

3. A number of diagenetic reactions in the mat sequence, such as preferential degradation of lower *n*-alkanes and *n*-alkenes. In contrast the mid-chain methyl branched alkanes originating from cyanobacteria appear to persist with depth in the mat, relative to *n*-alkanes. Preferential formation of C_{27} sterenes is also observed.

4. A natural, rather than anthropogenic, UCM is seen in the photosynthetic bacterial layer of the mat.

References

1. R. P. Philp, In: *Biogeochemistry of ancient and modern environments* (eds. P. A. Trudinger, M. R. Walter and B. J. Ralph) pp. 201–210, (Aust. Acad. Sci., Canberra,, 1981).
2. J. Trichet, In: *Advances in Organic Geochemistry*, 1966 (eds. G. B. Hobson and G. C. Speers), pp. 265–284, (Pergamon Press, Oxford, 1970).
3. C. Defarge, Contribution à l'étude géochimique et pétrologique des formations protostromatolitiques de Polynésie. Application à la connaissance des mécanismes de la précipitation des carbonates de calcium au sein de matières organiques sédimentaires. Thèse de Doctorate de spécialité. Université d'Orléans (1983).
4. C. Defarge and J. Trichet, *C. R. Acad. Sci. Paris* **299**(II), 11, 711–716 (1984).
5. J. Trichet, *C. R. Acad. Sci.*, Sér D. **265,** 1464–1467 (1967).
6. J. R. Disnar, J. R. and J. Trichet, *Geochim. Cosmochim. Acta* **45,** 353–362 (1981).

7. S. C. Brassell, A. P. Gowar and G. Eglinton, In: *Advances in Organic Geochemistry,* 1979, (eds. A. G. Douglas and J. R. Maxwell), pp. 421–426 (Pergamon Press, Oxford, 1979).
8. R. P. Philp, S. Brown, S. Calvin, S. Brassell and G. Eglinton, In: *Environmental Biogeochemistry and Geomicrobiology,* 1, (ed. W. E. Krumbrein), pp. 255–270 (Ann Arbor Science, 1978).
9. J. Han and M. Calvin, *Proc. Nat. Acad. Sci. U.S.A.* **64,** 436–443 (1969).
10. J. Oro, T. G. Tornabene, D. W. Nooner and E. Gelpi, *J. Bacteriol.* **93,** 1811–1818 (1967).
11. A. S. Mackenzie, S. C. Brassell, G. Eglinton and J. R. Maxwell, *Science* **217,** 491–504 (1982).
12. K. L. Edmunds, Organic geochemistry of lipids and carotenoids in the Solar Lake microbial mat sequence. Ph.D. Thesis, University of Bristol (1982).
13. J. J. Boon, H. Hines, A. L. Burlingame, J. Klok, W. I. C. Rijpstra, J. W. de Leeuw, K. E. Edmunds and G. Eglinton, In: *Advances in Organic Geochemistry,* 1981, (ed. Bjoroy *et al.*), pp. 207–227 (Wiley and Sons, New York, 1983).
14. E. H. Gelpi, H. Schneider, J. Mann and J. Oro, *Phytochemistry* **9,** 603–617 (1970).
15. W. Giger, C. Schaffner and S. G. Wakeham, *Geochim. Cosmochim. Acta* **44,** 119–129 (1980).
16. P. W. Brooks, G. Eglinton, S. J. Gaskell, D. McHugh, J. Maxwell and R. P. Philp, *Chem. Geol.* **20,** 189–204 (1976).
17. J. G. Jones, *J. Soil Sci.* **21,** 330 (1970).
18. B. M. Didyk, B. R. T. Simoneit, S. C. Brassell and G. Eglinton, *Nature* **272,** 216–222 (1978).